**MAPPING STRATIGRAPHIC LAYERS OF EXPOSED IMPACT CRATERS ON THE EDGE OF VALLES MARINERIS** L. X. Rader[1], B. J. Thomson[2], C. I. Fassett[3], R. A. Beyer[4], and M. D. Dyar[1]. [1]Dept. of Astronomy, Mount Holyoke College, South Hadley, MA 01075, rader22l@mtholyoke.edu, [2]Dept. of Earth and Planetary Sciences, University of Tennessee, Knoxville, TN 37996, [3]NASA Marshall Space Flight Center, Huntsville, AL 35805, [4] Sagan Center at the SETI Institute, Mountain View, CA, 94043.

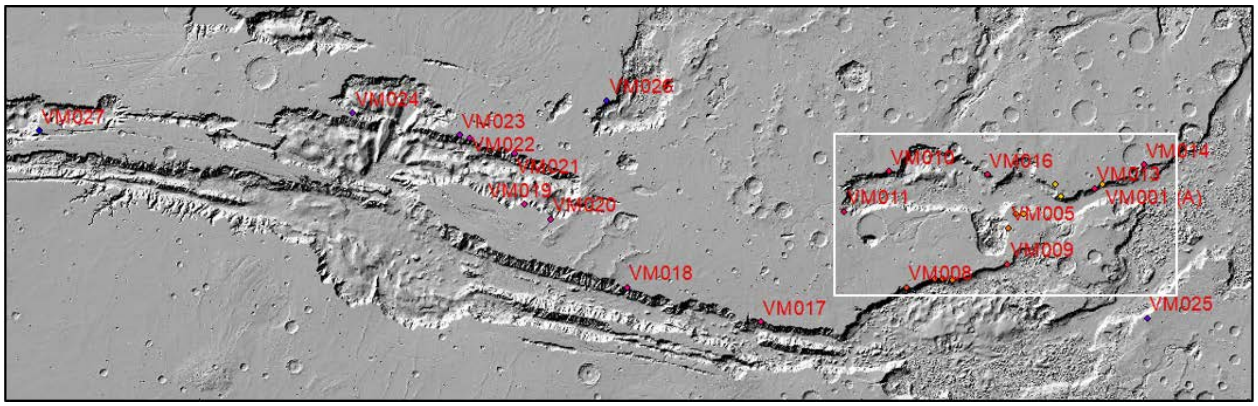


**Figure 1.** Valles Marineris with all of the locations identified as cut craters labeled in red. Preliminary studies have been done of VM001, VM003, VM006, VM007, VM014, VM017, VM019, and VM027. This study focuses primarily on VM007.

**Introduction and Background:** Observations of impact craters on planetary bodies are primarily conducted using surficial analysis [1-4]. Interpretation of the subsurface beneath craters is thus commonly limited to what can be indirectly inferred from data about their surface structure, for example, from altimetry data [5-7]. On Mars, a population of craters on the edge of Valles Marineris has been exposed in cross-section due to erosion and tectonic activity. These "cut craters" provide an opportunity to examine the subsurface of the impact craters and the surrounding target material directly.

Cut craters (**Figures 1, 2**) previously identified for this study by Bradley Thomson and James Huntington are exposed via lateral erosion and backwasting, exposing layers in the subsurface that can be mapped to determine characteristics of both the impact crater and the target material [8]. Layers (where present) are exposed on the canyon walls, allowing for a more complete understanding of the subsurface both inside and outside the cut craters in a manner similar to classic small-scale impact experiments into layered sand [9].

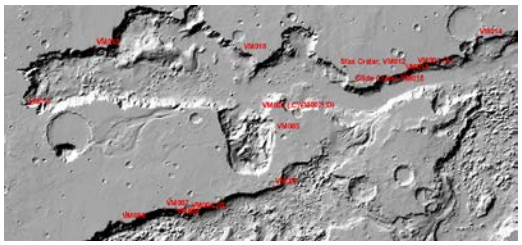

**Figure 2**. White rectangle enlarged from Figure 1.

**Methods:** Stereo pair images from the HiRISE instrument on the Mars Reconnaissance Orbiter (MRO) [10] were used to construct digital elevation models (DEMs) of previously identified cut crater locations [8] using the Ames Stereo Pipeline [11, 12]. The DEMs of each cut crater were imported into ArcGIS, and then subsurface layers were mapped by visual identification [8] (**Figure 3**). Each layer mapped was regionally named by the location around the crater where it is observed, then converted to discrete points. Elevations were acquired for each point in each mapped layer of a cut crater location, then coupled with the *x* and *y* coordinate values, before importing into MATLAB [8]. A surface-fitting routine was then used to identify the best-fit plane to each set of points, allowing each layer to be isolated and observed.

**Observations and Conclusions:** The mapped layers show primary characteristics of the subsurface layers of the cut crater. In the crater VM007 (**Figs. 2 and 3**), the layer in MATLAB illustrates the angle of the subsurface layer, from which layer thickness, rim uplift, and ejecta properties can be determined. The mathematically produced layers also provide insight into the overall nature of the geometry of the VM007 layers.

The rim to rim diameter of VM007 is 2.36 km while the observable crater rim edge extends farther into Valles Marineris. The mapped layers exist beneath the crater are exposed and have a greater strength than the surrounding rock that has been eroded down forming Valles Marineris. The upper edge of Valles Marineris has a similar shape to both lower layers, which implies

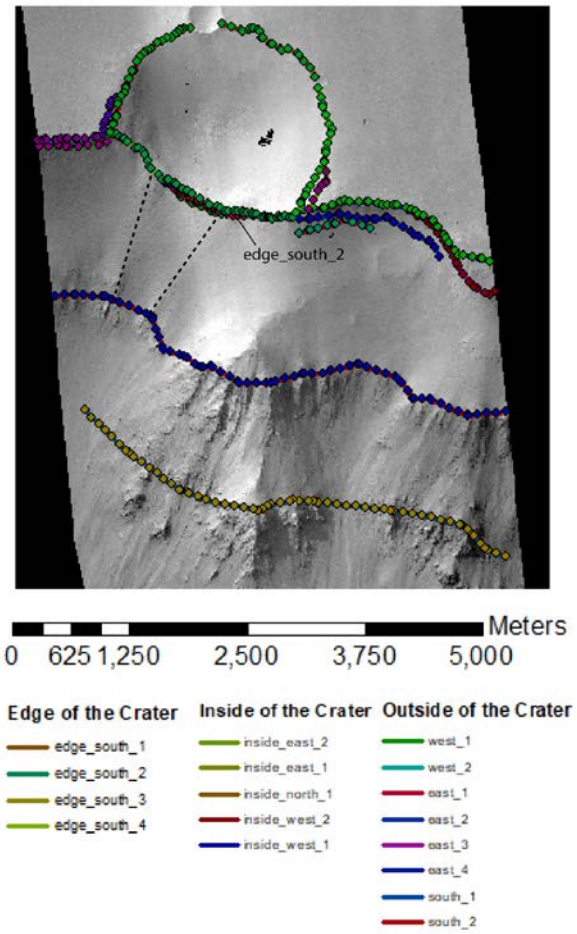


**Figure 3.** HiRISE stereo pair ESP_018940_1680 and ESP_025599_1680. DTM and Digital Raster Graphic (DRG) created for cut crater location VM007 with mapped layers. Visible dots on the lines indicate the points overlain onto the layers. Black lines indicate stronger rock formations under surface layer of target material.

that the target material of the crater has a similar strength to the lower layers that resisted the erosion. Particularly when observing the subsurface layer "east_3", evidence for a more rigid layer is shown, resisting the erosion. Layer "edge_south_2" occurs closely beneath the rim of the crater, has been affected by the older, lower layers. While the crater is significantly younger than the lower mapped layers, the stronger rock structures observed must be taken into account when analyzing layers for thickness and structural geometry when examining the effect of the impactor.

**Future Work**: This study establishes the foundational workflow needed to analyze cut crater locations. The example presented illustrates how the mapped layers can provide valuable insight into the primary characteristics of the cut craters and subsurface layers [13].

The work can also deepen the overall understanding into the stratigraphy of the rock layers after an impact and the effects of degradation on both the ejecta and target material [14]. This study presents an early state of research that can be used to understand the population of impact craters that exhibit a cross section exposed, including but not limited to the already identified cut crater locations in this research [8, 11]. This crater population can be used to gain a deeper insight into the target rock and how the existing layers of rock reacted to the impact can be seen from the observed layers [13, 14]. The study of impact cratering can also be used to understand the morphology of planetary surfaces by examining the exposed subsurface layers of cut craters and more can be learned about erosional properties of martian impact craters.

**Acknowledgements:** This work was partially supported by NASA MDAP award NNX11AN01G to BJT and RAB.

**References:** [1] Chapman C. R. et al. (1974) *Icarus*, 22, 272-291. [2] Barlow N. G. and Bradley, T. L. (1990) *Icarus*¸87, 156-179. [3] Grant J. A. and Schultz P. H. (1993) *JGR*, 98, 11025-11042. [4] Hartmann W. K. (1971) *Icarus*, 15, 410-428. [5] Smith D. E. et al. (1999) *Science, 284*, 1495-1503. [6] Watters W. A. et al. (2011) *Icarus, 211*, 472-497. [7] Wray J. J. et al. (2008) *Geophys.Res. Letts., 35*, L12202. [8] Thomson B. J. (2006) *LPS XXXVII*, abstract #1906. [9] Stoffler, D. et al. (1975) *JGR, 80*, 4062-4077. [10] McEwen A. S. et al. (2007) *JGR, 112*, E05S02. [11] Beyer, R. A. et al. (2017). NeoGeographyToolkit / Stereo Pipeline v2.6.0. DOI: 10.5281/zenodo.581187. [12] Moratto, Z. M., et al. (2010) *LPS XLI*, abstract #2364. [13] Kruger T et al. (2017) *Meteor. Planet. Sci., 52*, 2220-2240. [14] Strum S. et al. (2016) *JGR Planets, 121*, 1026-1053.